Science of the Total Environment 814 (2022) 152660

Contents lists available at ScienceDirect

Science of the Total Environment

journal homepage: www.elsevier.com/locate/scitotenv

Research Paper

Survival and activity of an indigenous iron-reducing microbial community from MX80 bentonite in high temperature / low water environments with relevance to a proposed method of nuclear waste disposal

Katie A. Gilmour [a,*,1], Colin T. Davie [a], Neil Gray [b]

[a] School of Engineering Newcastle University, NE1 7RU, United Kingdom
[b] School of Natural and Environmental Sciences, Newcastle University, NE1 7RU, United Kingdom

HIGHLIGHTS

- Microbial communities were characterised following incubation in desiccated MX80 bentonite.
- Geomechanical properties and mineralogical changes of MX80 bentonite were analysed.
- Microbial activity may act to indirectly inhibit corrosion of steel waste canisters in contact with MX80 bentonite.
- Microbially influenced mineralogical changes may lead to a decrease in swelling.
- Microbes are active and can survive in desiccated, high temperature MX80 bentonite.

GRAPHICAL ABSTRACT

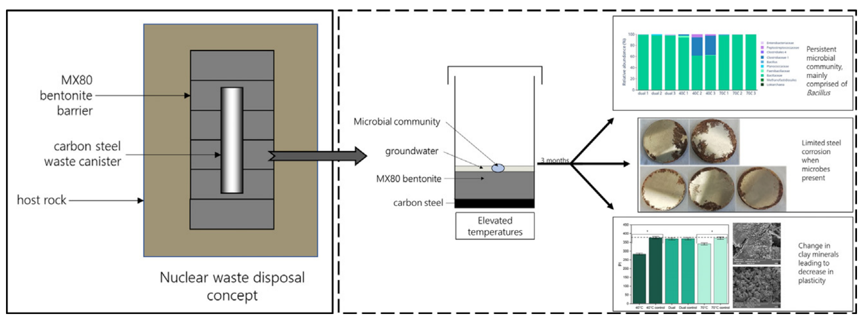

ARTICLE INFO

Article history:
Received 7 October 2021
Received in revised form 19 December 2021
Accepted 20 December 2021
Available online 24 December 2021

Editor: Frederic Coulon

Keywords:
Bacteria
Bentonite
Deep geological disposal
Iron-reduction
Clay minerals
Desiccation

ABSTRACT

MX80 bentonite clay has been selected as the buffer and backfill in a proposed method for long-term deep geological storage of nuclear waste. Extensive studies have been carried out on the geomechanical properties of the clay; however, it is not clear what effect microbes, specifically iron-reducing bacteria, will have on its ability to function as an affective barrier. Iron-reducing bacteria can reduce structural or external Fe(III) to Fe(II) and have been previously identified in the indigenous microbial community of MX80 bentonite. Experiments to assess bacterial survival at the high temperature and low water conditions likely to exist in the repository were carried out at different temperatures with the addition of steel to represent a nuclear waste canister. The resulting microbial enrichments were analysed, and mineralogical and geomechnical analysis was carried out on the clay. Microbial sequencing revealed that iron-reducing bacteria, and other indigenous species can survive these conditions in MX80 bentonite in either an active or dormant state. Microbial influenced mineralogical changes may lead to a loss of silica from the clay and reduction of Fe(III) to Fe(II). These changes could alter the ability of the clay to act as an effective barrier in nuclear waste disposal. Furthermore, evidence of reduced steel corrosion when microbes were present suggested that microbial activity may lead to either a protective coating on the steel or depletion of oxygen to slow corrosion. The production of such a layer would benefit nuclear waste disposal by inhibiting corrosion of a metal waste canister.

* Corresponding author.
E-mail address: katie.gilmour@northumbria.ac.uk (K.A. Gilmour).
[1] *Currently at:* Hub for Biotechnology in the Built Environment, Department of Applied Sciences, Faculty of Health and Life Sciences, Northumbria University, Newcastle upon Tyne, NE1 8ST, UK

http://dx.doi.org/10.1016/j.scitotenv.2021.152660

1. Introduction

Deep geological storage is an option for high-level nuclear waste (HLW) disposal, which is being considered by countries across the world, including the UK (Arlinger et al., 2013; IAEA, 2018; NDA, 2010). Plans are in various stages of completion with several designs based on the KBS-3 (kärnbränslesäkerhet-3) design from SKB (Swedish Nuclear Fuel and Waste Management Co - Svensk Kärnbränslehantering AB) (Aunqué et al., 2006). The design features a metal canister encasing the vitrified nuclear waste that is surrounded by a clay barrier. This barrier acts as an infill between the canister and the host rock and due to the low hydraulic conductivity and ability to act as a sorbent to cationic radionuclides (Kuleshova et al., 2014), will limit the migration of radionuclides in event of a breach. The swelling pressure of the MX80 bentonite is also critical in the repository design, as is the clay plasticity, as the clay will respond to changing moisture contents without cracking or allowing the canister to sink. More specifically, the UK design is likely to consist of a carbon steel canister encasing the waste with an MX80 bentonite clay barrier all buried to a depth of 1000 m below the surface (NDA, 2016; NDA, 2010). There are microbial communities associated with MX80 bentonite, as well as groundwaters and host rocks (Chi and Athar, 2008; Hallbeck and Pedersen, 2012; Povedano-Priego et al., 2020; NDA, 2016; Smart et al., 2017; Gilmour et al., 2021). Therefore, in addition to the materials in the repository design and the potential abiotic reactions that could occur, microbes will also be present and microbially influenced reactions must also be considered.

The lifespan of multi-barrier HLW repositories is 10,000–100,000 years (Yang et al., 2019). After closure of the repository there are predicted phases of confinement. Specifically, in the Nagra (the Swiss national radiowaste management organisation) design, the temperature will increase from 40 to 50 °C in a gradient across the clay barrier up to 100 °C at the canister surface by year 50 after closure (Landlot et al., 2009). Indeed, 100 °C is largely reported as the maximum tolerable temperature for the bentonite barrier as experiments have found that prolonged exposure to high temperatures results in a decrease in swelling pressure (Svensson et al., 2011). This initial phase of repository closure will be coupled with a decrease in water activity. During this initial phase there will also be an evolution to anaerobic conditions. However, by year 100 post-closure, the temperature across the barrier will have decreased to, and is likely to remain at, 40–50 °C and groundwater may begin to re-saturate the barrier. The UK concept is likely to have a similar temperature evolution (RWM, 2016), which suggests the maximum temperature at the host rock / clay interface will be 70 °C by year 50, with the long-term temperature being 40 °C. Not only does this environment allow for microbial growth of some thermophilic species, but this interface may also have more space than elsewhere in the repository to allow for this growth. For example, there may be some gaps where the bentonite has not fully swelled tightly to the host rock surface (Wilson et al., 2010; Stroes-Gascoyne et al., 2011). Indeed, Jalique et al. (2016) found that whilst microbial growth was limited in a highly compacted clay barrier after eight years, there were microbes at the clay / host rock interface. Furthermore, the MX80 bentonite backfill that is not as highly compacted may also allow for microbial growth (NDA, 2016).

The clay barrier must be able to respond to changing conditions within the repository such as temperature and moisture content without compromising the barrier performance. Therefore, specific geomechanical properties make some clays more suited to this design. Namely, a high swelling ability; high plasticity; low porosity; low hydraulic conductivity; and high thermal conductivity (Sellin and Leupin, 2013; Wilson et al., 2010). Highly compacted Wyoming MX80 bentonite has been widely proposed for use as a clay barrier – and backfill – for repositories, as it possesses all these characteristics (NDA, 2016; Jönsson et al., 2009; Bradbury et al., 2014; Kiviranta and Kumpulainen, 2011). Additionally, the low porosity of the clay in a compacted state results in an average micro (intra-aggregate) pore size of ≤ 0.02 μm when compacted at a range of dry densities (dry density = $\geq$ 1.6 Mg/m^3) (Bengtsson et al., 2015; Wang et al., 2016; Jalique et al., 2016). This pore size is thought to limit radionuclide transport in the event of a breach in a metal canister and will limit microbial activity within the buffer (West et al., 2002; Rättö and Itävaara, 2012). The required properties of a barrier clay, as described above, are dictated by its mineralogical composition and with respect to MX80 bentonite the montmorillonite content (80%) is important in ensuring the correct swelling pressure for the repository.

In addition to the predominantly montmorillonite content of MX80 bentonite there are other components present that may have an impact on how the clay performs in the repository. Namely, iron-bearing silicate minerals that have potential microbial interactions. There are several iron-containing minerals present and iron accounts for ~4% wt. of the MX80 bentonite (Karnland, 2010) with ~20% of this iron estimated to be Fe (II) and the remainder Fe (III). Furthermore, in the UK design, increased Fe (II/III) could be introduced to the clay as corrosion of the carbon steel canisters progresses (Bradbury et al., 2014; Necib et al., 2017; Davies et al., 2018). Therefore, the environment could selectively promote the growth of iron-interacting bacteria. In addition, MX80 bentonite contains 0.11–0.4% wt. organic carbon, which has been considered adequate to support microbial life (Sauzeat et al., 2001), albeit that a more recent assessment has shown that it is mostly inert (Marshall et al., 2015).

Iron-reduction within the clay, whether abiotic or microbially influenced, could result in an increase in non-swelling Fe (II) rich phyllosilicate minerals (Bradbury et al., 2014; Kim et al., 2004) either through indirect interactions with microbially excreted metabolites and H^+ or by dissimilatory iron-reduction (Uroz et al., 2009; Konhauser, 2007). Indirect interactions would allow more widespread reduction to take place, rather than localised reactions at sites where microbes are able to proliferate. Such mineralogical changes could result in alterations to the geomechanical properties of the clay, specifically a decrease in swelling that could result in a higher hydraulic conductivity or lower plasticity and sealing capacity (Sahin et al., 2011; Glatstein and Francisca, 2014; Stucki et al., 2009).

Previously, microbial communities capable of reducing iron have been identified in MX80 bentonite, and in the groundwater at international repository sites (NDA, 2016; Svemar et al., 2016; Gilmour et al., 2021). Furthermore, concerns have been raised about the possibility of microbially induced corrosion (MIC) accelerating the corrosion of the waste canisters. Indeed, several studies demonstrate the ability of iron-oxidizing bacteria and sulphate-reducing bacteria (SRBs) to corrode metal including carbon steel (Pedersen et al., 2017; Svensson et al., 2011). There are several iron-interacting bacteria that either oxidise elemental iron or Fe (II) to Fe (III) (Singh et al., 2018; Konhauser, 2007) or reduce Fe (III) to Fe (II) (Morgado et al., 2012; Fan et al., 2018).

Experiments to test the survivability of microbes in repository environments have so far focused largely on temperature alone, and mainly with specific bacteria rather than the viable indigenous community that it has been recently shown contains putative thermophiles and spore-forming bacteria (Gilmour et al., 2021). Pedersen (2012) found that spore-forming SRBs from bentonite can survive 80 °C, however, they were not active and only a small percentage survived. Further experiments by Masurat et al. (2010) also found a decrease in the viability of SRBs when bentonite samples were exposed to 120 °C for 20 h. Stroes-Gascoyne et al. (2002) found, following re-saturation, that the viability of microbes in MX80 bentonite was preserved under dry conditions (18% moisture content), however, heat was not considered.

Therefore, it is clear from earlier studies that, specifically, SRBs indigenous or introduced to MX80 bentonite can tolerate elevated temperatures, or low water environments (Pedersen et al., 2017; Masurat et al., 2010; Stroes-Gascoyne et al., 2002). However, the exact conditions likely to be faced in the repository (elevated temperatures combined with low water activity) have not been fully investigated, nor has the survivability of an indigenous iron-reducing microbial community. Previously, it has been shown that iron-reducing bacteria (IRBs) native to MX80 bentonite can reduce structural iron within the MX80 bentonite and contribute to MIC (Kim et al., 2004; Lantenois et al., 2005). However, it is not clear what effect these biogenic activities have on the geomechnical properties of the clay in conjunction with survival at elevated temperatures in low water conditions. The aim of the study described below was to assess the survivability of the indigenous, viable iron-reducing community previously enriched from MX80 bentonite (Gilmour et al., 2021) in desiccated, high temperature conditions, and including the presence of steel to simulate the waste canister. These experiments also assessed what biologically driven changes may have occurred mineralogically and geomechanically to the MX80 bentonite during this process.

2. Materials and methods

2.1. Details of the MX80 bentonite clay used in enrichment experiments

Compacted Wyoming MX80 bentonite blocks were sourced from SKB's (Svensk Kärnbränslehantering AB - Swedish nuclear waste management organisation) supplier (ClayTech AB®) (27% wt. water = 97% saturation, 1.56 Mg/m^3 dry density, corresponding to a swelling pressure of 4–5 MPa (Börjesson, 2010)). The mineralogical composition of this bentonite is presented by Karnland (2010). An average of 6 samples comprised 81.4% montmorillonite, 0.9% low-cristobalite, 3% quartz, 0.9% gypsum, and 13.8% other (inclusive of 4% wt. iron). Bentonite disks measuring 60 × 15 mm were cut from the compacted blocks using a core drill.

2.2. Details of S275 steel

A 1 m cylinder, 60 mm diameter of S275 steel was sourced from Metal Supermarkets UK (known globally as The Convenience Stores for Metal™). The composition of S275 is defined as <0.25% carbon, <0.05% sulfur, <0.05% silicon, <1.6% manganese, and < 0.04% phosphorus. S275 carbon steel coupons measuring 60 × 5 mm were cut using a lathe and then smoothed using a surface grinder. Coupons were then left in oil to prevent rust and cleaned with acetone immediately before sterilisation.

2.3. Composition of synthetic groundwater

A Sellafield-like groundwater was used as a proxy in these experiments because it is representative of UK groundwaters as well as being of similar composition to other groundwaters used in experiments pertaining to nuclear waste repositories (Baker et al., 1997; Gilmour et al., 2021; Fraser Harris et al., 2015; Schäfer et al., 2004). Synthetic Sellafield-like groundwater (Wilkins et al., 2007) composed of (g/L) KCl, 0.0066; $MgSO_4.7H_2O$, 0.0976; $MgCl_2.6H_2O$, 0.081; $CaCO_3$, 0.1672; Na_2SiO_3, 0.0829; $NaNO_3$, 0.0275; NaCl, 0.0094; $NaHCO_3$, 0.2424 was enriched with 12 mg/L acetate (sodium acetate trihydrate). This concentration of organic carbon was chosen because it reflects that which has been found to be naturally occurring in groundwater at international repository sites (Pedersen, 2012; Kotelnikova and Pedersen, 1998). Acetate is thought to be the most abundant carbon source in these groundwaters due to the presence of lytic phages (Kyle et al., 2008) and associated processes, known as a viral shunt, which generates short chain organic acids (Suttle, 2007).

2.4. Preparation of the microbial community inoculum

Previously, iron-reducing microbial enrichments of compacted MX80 bentonite were carried out (Gilmour et al., 2021). The resulting microbial community, composed largely of *Bacillus* and *Clostridia* species (>95% relative abundance) and including known iron-reducers (e.g. *Desulfosporosinus* and *Desulfitobacterium*), was stored in glycerol stocks at −80 °C. Stocks were thawed and grown under anaerobic conditions (vinyl anaerobic chamber, Coy Lab Products, 5% H_2: 95% N_2) at 20 °C in 15 mL synthetic groundwater with organic enrichment as described in Gilmour et al., 2021. After 10 days growth, cell counts using SYBRGold were carried out to confirm adequate growth using a fluorescence microscope (Olympus BX40 Epi-fluorescence microscope).

2.5. Desiccation experimental method

MX80 bentonite disks were heated in a dry oven at the relatively low temperature of 40 °C for 48 h to prevent cracks that developed during rapid high temperature drying. Sterilisation took place by placing MX80 bentonite disks on top of steel coupons in Nalgene jars (60 mm diameter), which were heated to 105 °C in a dry oven for 48 h (Fig. 1). Previous experiments showed that this method is adequate for sterilisation of these compacted blocks of MX80 bentonite (Gilmour et al., 2021). In order to ensure any changes to the clay observed during the experiment were not due to drying through the sterilisation process, all samples were sterilised and biotic experiments were later re-inoculated.

Following sterilisation, 8 ml of acetate amended Sellafield-like groundwater was added (27% moisture content -equal to the moisture content of the as received clay blocks prior to heat sterilisation). After 24 h some jars were inoculated with 50 μl of the iron reducing / fermentative MX80 bentonite bacterial consortium stocks (6×10^5 cells/mL). The inoculation site was the centre of the bentonite surface furthest from the steel (Fig. 1). Control jars were not inoculated.

Three inoculated and three control jars were then incubated at 40 °C or 70 °C for 16 weeks. Lids were screwed on but were not airtight to allow water evaporation to occur and desiccation to develop. A further experiment with three inoculated replicates and controls was also included, this experiment was incubated at 70 °C for 8 weeks and then cooled to 40 °C (temperature decreased 1 °C per day for 30 days) before a final incubation at 40 °C for 4 weeks. 40 °C was chosen as the lowest temperature as it represents the expected temperature of the clay/host rock interface for the majority of the duration of repository closure in the UK concept (RWM, 2016). Similarly, 70 °C was chosen as it represents the highest expected interface temperature (RWM, 2016). Although initially oxic, it is believed that the clay will limit oxygen diffusion to the steel and an anoxic or micro-oxic state will develop. At the end of the experiment, the steel coupons were recovered and photographed. ImageJ (version 1.52d) was used to analyse the area of the surface of the steel at the steel/clay interface that had corroded as a percentage of the total area.

2.6. Plasticity index testing

The plasticity index (PI) of MX80 bentonite used in desiccation tolerance and temperature tolerance experiments was measured before and after the experiment as per the British Standard (Institution, 1990) method (BS:1377: 1990: Part 2, section 3.4, 3.5). The PI was determined as the difference between the plastic limit and the liquid limit. Briefly, the plastic limit was calculated as the % moisture content of the clay when a hand rolled cylinder of it begins to shear longitudinally and transversely at a diameter of 3 mm. The liquid limit was determined using the four-point cone penetrometer method. The % moisture content of the clay relating to four different penetration depths was measured and thus the % moisture content at 20 mm penetration was calculated. Additionally, 10 g of MX80 bentonite was used to determine the % moisture content of the MX80 bentonite immediately after the experiment. This measurement was taken as described in BS:1377: 1990: Part 2, section 2.3 (Institution, 1990).

2.7. Mineralogical analysis of MX80 bentonite

1 g MX80 bentonite from the centre of the clay was dried under anoxic conditions (5% H_2: 95% N_2) for a minimum of ten days prior to X-ray diffraction (XRD) analysis. Samples were hand ground with a pestle and mortar and run (PANalytical X'Pert Pro Multipurpose Diffractometer) using Cu as the target metal, as standard, (λ = 0.154 nm) for 5 h. Spectra were obtained as .raw files and analysis including mineral identification and spectrum fitting was completed using HighScore Plus. Initially, the background was subtracted, and peaks were identified using tools in the program. Further peaks and shoulders were

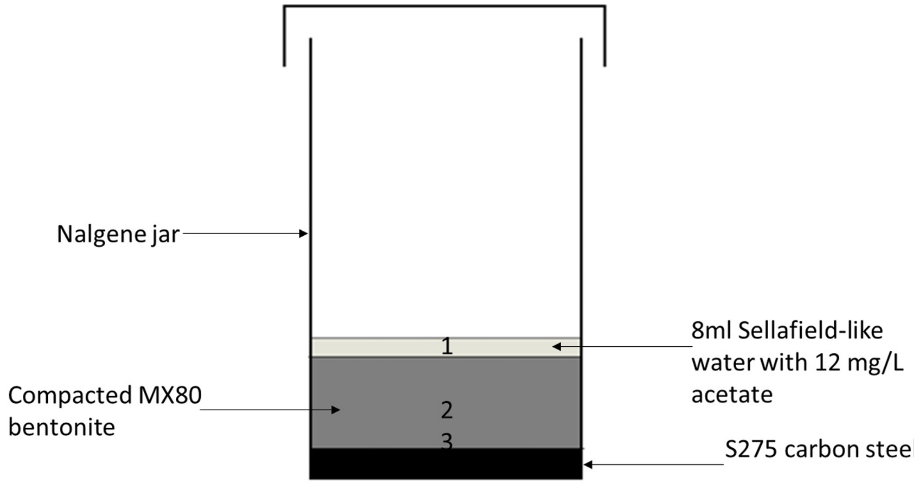

Fig. 1. Schematic of desiccation tolerance experiments. The site of inoculation (1), XRD and microbial sequencing sampling (2) and the sampling site for SEM images (3) is shown.

picked out manually. As part of this analysis, identified peaks were characterised using mineral databases; ICDD 1999 and COD 2016. Reitvald refinement was run in HighScore Plus to ensure a good fit (Chi Square = ≤8).

Additionally, 0.5–1 g MX80 bentonite was recovered from the steel / clay interface and dried anoxically (5% H_2: 95% N_2) for scanning electron microscopy imaging (SEM) (Tescan Vega 3LMU). Samples were mounted on aluminium stages using carbon tape and silver paint. Samples were then coated with gold by Electron Microscopy Research Services (Newcastle University) prior to imaging.

2.8. DNA extraction and bacterial community structure analysis

At the completion of the experiment, DNA extraction was performed on all the replicates of desiccation and temperature tolerance experiments. A PowerSoil DNA isolation kit (MoBio) was used with 0.5 g of MX80 bentonite taken from the centre of the MX80 bentonite – a location spatially distant from the site of inoculation (Fig. 1). DNA was extracted according to the manufacturer's instructions, except that the final DNA elution step was performed with 50 μL instead of 100 μL elution buffer. DNA extractions were confirmed and quantified using QuBit.

DNA extracts were then sent to NU-OMICS, Northumbria University, where amplicons were generated for 16S rRNA gene Illumina sequencing of the V4 variable region (Kozich et al., 2013). Raw sequencing data (FastQ files) obtained from the Illumina sequencing platform were then demultiplexed and analysed as part of the QIIME 2 pipeline (Caporaso et al., 2010) using DADA2 for ASV (amplicon sequence variant) selection (Callahan et al., 2016). ASVs which appeared in the negative control were removed from the other samples. Phylogenetic trees were constructed using representative sequences of dominant taxonomic groups. Trees were produced by using BLASTN (Zhang et al., 2009) to identify nearest neighbours and subsequently alignment and similarity value calculations were performed using MEGA7 via the neighbour-joining method of Saitou and Nei (1987) and bootstrap values were determined according to Felsenstein (1987).

2.9. Significance testing:

A one-way ANOVA was used (RStudio Team, 2020) to test for significance of these results between abiotic and live controls as well as between temperature treatments. *P*-values were obtained following normality checks, and post-hoc Turkey tests were carried out.

3. Results

3.1. Plasticity measurements of the MX80 bentonite from desiccation and temperature tolerance experiments

The plasticity index (PI) of the MX80 bentonite significantly changed during the experiment, at 40 °C and 70 °C, when microbes were present (Fig. 2). The PI is calculated from two parameters, namely the plastic limit (PL) and liquid limit (LL) (PI = PL-LL). While the PL was unchanged (between 30 and 39% moisture content across all samples) it was the LL that was lower in the presence of microbes. More specifically at 40 °C with microbes; the PI was 283 compared to 376 for the abiotic control ($p = 0.017$), and 379 for the PI before the experiment. The PI of the MX80 bentonite incubated at 70 °C with microbes was 346, which was also significantly lower when compared to the abiotic control ($p = 0.0276$). There was no significant difference in PI in the dual temperature experiment when microbes were present. There was no significant difference between the abiotic controls at different temperatures, and a

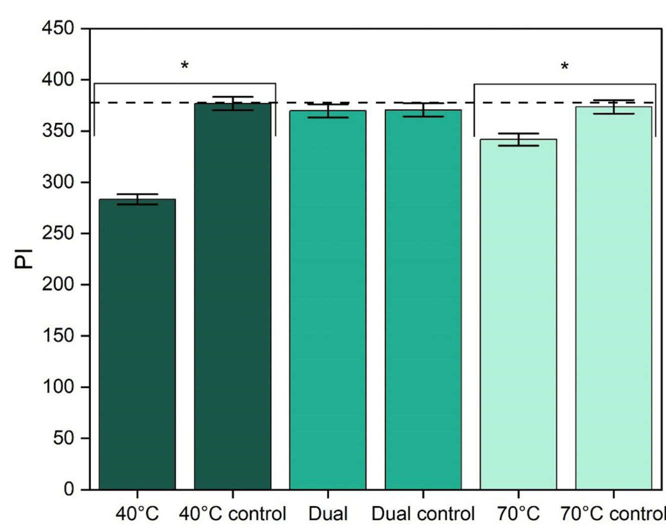

Fig. 2. PI of MX80 bentonite recovered from desiccation tolerance experiments at different temperatures. Dotted line indicates PI of MX80 bentonite before the experiment. Error bars represent standard error, stars represent statistically significant differences in PI (* $p < 0.05$; ** $p < 0.01$; *** $p < 0.001$).

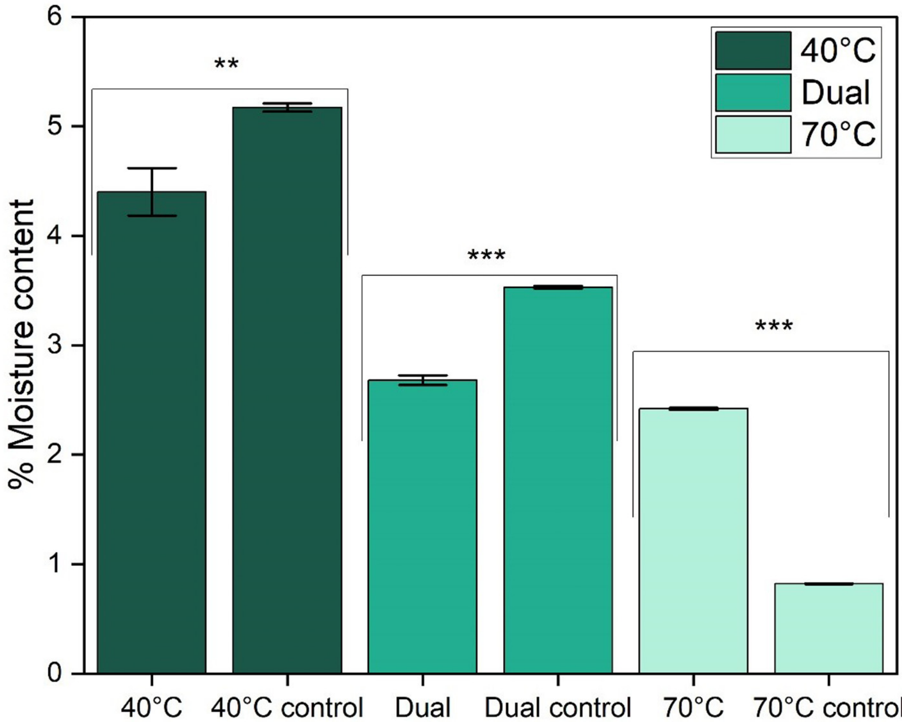

Fig. 3. %moisture content of MX80 bentonite recovered from desiccation tolerance experiments at different temperatures. Error bars show standard error (n = 3) and stars represent statistically significant differences between the biotic experiment and abiotic control (* p < 0.05; ** p < 0.01; *** p < 0.001).

significant difference between microbial inoculated experiments at different temperatures ($p = 0.0348$).

Additionally, the %moisture content of the clay was calculated (Fig. 3). It was found that the experiments at higher temperatures had a lower moisture content than those at 40 °C and there was a progressive decline in temperature the longer the experiment were incubated at 70 °C. Furthermore, the % moisture content of the experiments at 70 °C were found to be significantly higher when microbes were present ($p < 0.001$). These results were found to be significantly lower when microbes were present at 40 °C ($p < 0.001$), and dual temperature ($p < 0.001$). Similarly, it was found that both microbial presence and higher temperature were significant factors in decreasing % moisture content ($p \leq 0.001$).

3.2. Mineralogical analysis of the MX80 bentonite from desiccation/temperature tolerance experiments

Mineralogical analysis of the clay samples from the different incubations identified some commonalities. All samples contained clay minerals known to exist in MX80 bentonite (Karnland, 2010) (quartz, montmorillonite, feldspar). However, the abiotic samples from the dual temperature control were also found to contain another member of the feldspar mineral series, not present in any other samples: anorthite ($CaAl_2Si_2O_8$). Although bulk XRD analysis is adequate to identify the iron oxide minerals present, there are limitations to the identification of clay minerals due to the interlamellar spacing. Therefore, limited conclusions can be drawn from the presence or absence of specific clay minerals such as anorthite. Differences between the mineralogy of the MX80 bentonite were observed, both between microbial and abiotic samples, and samples at different temperatures (Fig. 4); however, mineralogy was consistent across replicates. Notably, magnetite (Fe_3O_4) was identified in biotic samples from all incubation temperature regimens, but only in abiotic (control) samples at 70 °C. Other differences included the presence of a sodium iron oxide ($NaFeO_2$) at 40 °C and 70 °C incubations when microbes are present but not in abiotic controls. However, both the biotic and abiotic samples from the 70 °C incubation contained goethite (Fe(*III*)OOH).

Some changes to the bentonite surface were also observed in SEM images of MX80 bentonite from the steel / clay interface (Fig. 5). Extensive mineral precipitation was observed on the surface of MX80 bentonite from biotic experiments at 40 °C, which has been identified as low-cristobalite (images are comparable to those generated by Horwell et al. (2013)), and octahedral magnetite. However, other minerals may also be co-precipitated. Similar minerals were observed on the surface of MX80 bentonite from the biotic dual temperature experiments, but this was more localised. The samples analysed from MX80 bentonite from desiccation tolerance experiments at 70 °C with microbes indicated iron oxide formation on samples from the centre of the MX80 bentonite disk closest to the steel coupon, which could be the sodium iron-oxide identified in the XRD.

3.3. Visualisation of corrosion of steel coupon recovered from desiccation tolerance experiments

The steel coupons used in these experiments did not corrode extensively. This result has been largely attributed to the dry conditions of the experiment. However, some corrosion was observed, particularly around the edges. There was visually more surface corrosion observed on steel from abiotic experiments than from experiments with microbes. This difference was particularly clear on samples from 40 °C. Photographs of the steel coupons recovered from these experiments can be found in supplementary material (Fig. S1). ImageJ measurements of the area of the steel surface visually corroded suggested that this result was significant ($P = 0.0374$) with a mean of 14% of the surface area corroded in biotic samples, compared to 35% in abiotic samples.

3.4. Community analysis of the desiccation tolerance experiments at various temperatures

Nine 16S rRNA libraries were derived from sequencing outputs of the desiccation tolerance experiments at various temperature regimens. These library sequences have been deposited in the NCBI's Sequence Read Archive (SRA) available under BioProject PRJNA594313. The sequencing yielded

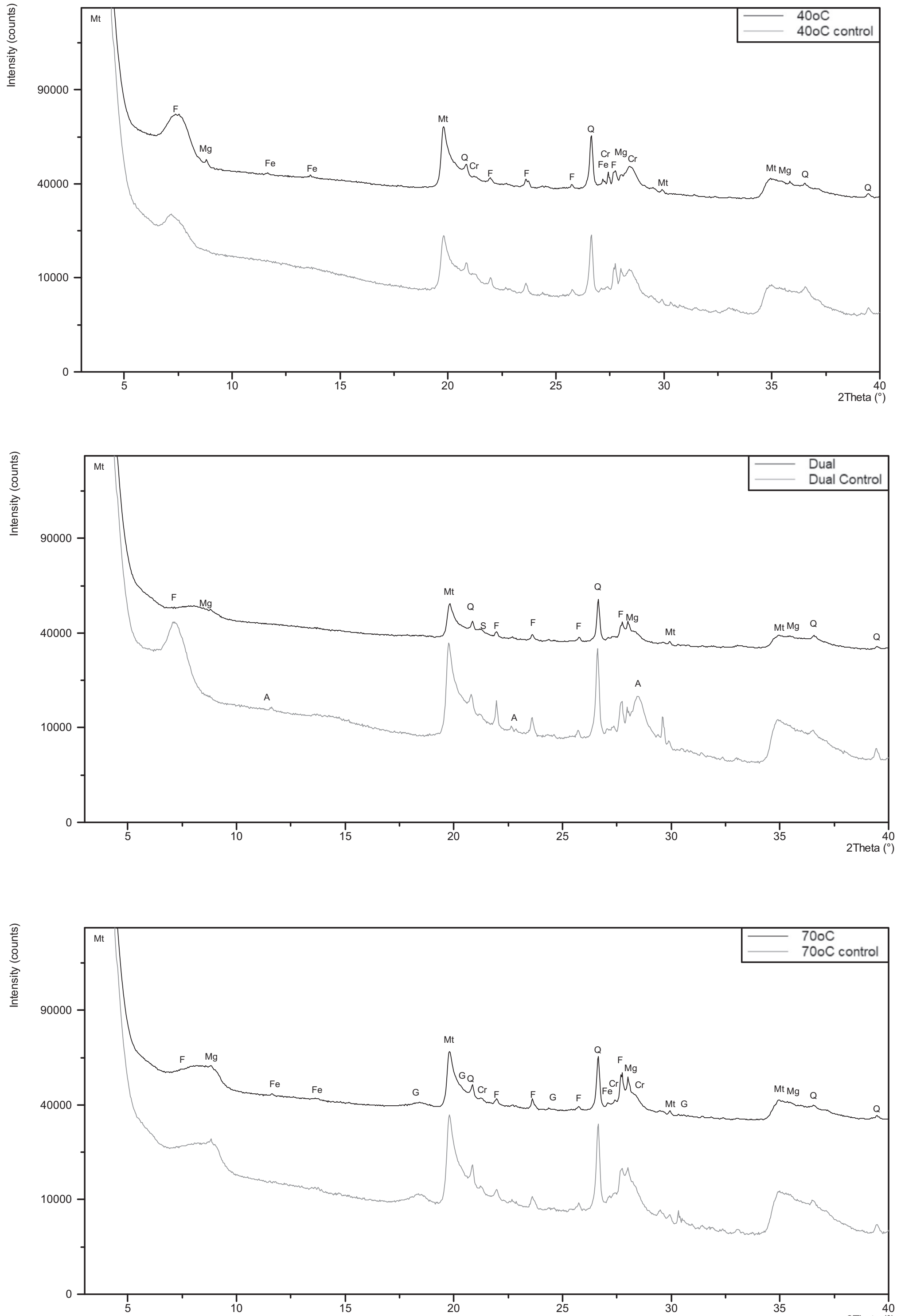

A	Cr	F	Fe	G	Mg	Mt	Q	S
Anorthite	Cristobalite	Feldspar	Sodium iron oxide	Goethite	Magnetite	Montmorillonite	Quartz	Sanidine

Fig. 4. XRD spectra of MX80 bentonite recovered from desiccation tolerance experiments were analysed using HighScore Plus. Images show raw spectra with key mineral peaks labelled.

average reads of 78,872 ± 3693 for 40 °C, 50,577 ± 7706 for dual temperature and 31,116 ± 9425 for 70 °C experiments; with an average read length of 227 bp across all libraries. The number of reads was significantly lower from the 70 °C libraries compared to the 40 °C ($p = 0.0435$). From this analysis, an average of 25 ± 7 (40 °C), 47 ± 3 (dual temperature), and 51 ± 9 (70 °C) ASVs were identified from the QIIME2 pipeline. Low sequence reads from control experiments and negative procedural sequencing controls indicate no contamination took place during the experiment or subsequently during DNA extraction and sequencing. The resulting libraries of enriched microbial communities of MX80 bentonite was largely composed of taxa assigned to the phylum firmicutes, most abundantly, taxa related to the genera *Bacillus* (Fig. 6). There was a significantly lower relative abundance of *Bacillaceae* at experiments run at 40 °C compared to those at higher temperatures ($p = 0.0236$).

However, there was also a substantially larger population of *Clostridaceae* species in the 40 °C experiment ($P = 0.0027$) in comparison to the relative abundance of *Clostridaceae* at other temperatures, which was found to be most closely related to *Clostridum beijerinckii* and *Clostridium subterminale* (fig. S2). Whereas ASVs identified from the dual temperature experiments were most closely related to solely *Bacillus* sp. and *Paenibacillus* sp. (fig. S3). It should also be noted that most of the nearest neighbour sequences identified by BLAST searches of NCBI database for the dual temperature experiments were isolated from high salinity environments such as salt lakes and marine sediments. This pattern of isolation source was similar for those sequences identified as nearest neighbours to the ASVs from the 70 °C experiments (fig. S4), however, salt tolerant species were more abundant in the dual temperature experiments. Similarly, this community was of lower diversity relative to the 40 °C incubation and was composed of mainly firmicutes, particularly *Bacillus*, albeit there was also a small population of gammaproteobacteria (comprising 0.1% relative abundance). As expected, due to the survival of spore-formers reported in previous experiments (Masurat et al., 2010; Stroes-Gascoyne et al., 2002) many species identified in these communities are putatively spore-formers, however, there are differences between the different temperature treatments. By considering all sequences that were able to be assigned to species level, 100% of species identified in the dual temperature experiments are putatively capable of forming spores compared to 98.2% of the community at 70 °C and only 83.72% of species at 40 °C.

4. Discussion and conclusions

There are several conclusions to be drawn from these desiccation and temperature tolerance studies. These conclusions are principally supported by the geotechnical and mineralogical data of the MX80 bentonite and further supported by the putative functions of the organisms identified in the microbial community.

It should be noted that bacteria added (from a previous enrichment of the same clay) to these experiments were of a higher initial concentration than would naturally occur in the MX80 bentonite and that the clay was not compressed in these experiments. Therefore, increased activity may have occurred relative to that possible in the repository where higher compaction, resulting in a lower pore size may contribute to decreased microbial activity. However, towards the end of the repository lifespan when the edges of MX80 bentonite have been eroded (Neretnieks et al., 2009; Börgesson et al., 2020) there may be potential for increased activity at the clay / host rock interface. Equally, some gaps may be present at this interface much earlier where the clay has not fully swelled allowing for some microbial growth (Wilson et al., 2010; Jalique et al., 2016; Stroes-Gascoyne et al., 2011).

During the repository lifespan, there may also be microbes introduced from other sources such as the local groundwater. The UK has not yet selected a repository site, so microbes from such a source have not been considered. Additionally, the radioactivity of the repository was not considered in these experiments, but may also inhibit the microbial community.

4.1. Survivability of indigenous bacteria of MX80 bentonite

To ensure DNA extracted from MX80 bentonite was indicative of an active bacterial population, a location spatially distant from the inoculation site was chosen for sampling. Previous attempts of amplification/sequencing of unenriched clay did not yield results (Stone et al., 2016; Poulain et al., 2008; Urios et al., 2012; Gilmour et al., 2021). Therefore, that growth must have occurred to have allowed colonization of the spatially separated site and the bacterial communities presented are representative of those able to survive in high temperature, low water conditions.

As expected, and observed in previous studies (Pedersen, 2012; Gilmour et al., 2021), many of the bacteria identified in the sequence libraries from the incubation experiments were putatively spore-formers, particularly in the higher temperature experiments. Spore-forming bacteria are able to withstand harsher conditions by entering a period of dormancy (Rättö and Itävaara, 2012). In this way, bacteria in the repository will be able to withstand the compaction process of the bentonite into blocks and the unfavourable habitat of the repository for decades and become active when conditions improve (e.g., as the temperature decreases, or groundwater becomes available). There was no significant differences observed in the microbial communities from replicates, which indicates that the community was uniform throughout the clay and that only a limited number of species were able to survive.

Many of the bacteria found to be present in the 40 °C community were closely related to those able to grow optimally at this temperature, and many more species indigenous to MX80 bentonite are also able to tolerate this heat (Gilmour et al., 2021). Interestingly, *Clostridia* were lost from communities subjected to the higher temperatures and do not survive to become active as the temperature cools (as illustrated in the dual temperature experiments), despite the ability for identified species to form spores (*C. beijernickii* (Patakova et al., 2019)). This may have be due to heat or low oxygen stress because many *Clostridia* are obligate anaerobes rather than *Bacillus,* which is a genus that is facultatively anaerobic. The higher temperatures may have accelerated drying conditions causing the clay to shrink from the edges and introducing a higher concentration of oxygen from the air.

The difference in community observed between the dual temperature experiments and 70 °C experiments is also interesting. It suggests that species such as *Lysinibacillus halotolerans* (a highly saline-tolerant species), and certain *Bacillus* sp. were likely only able to survive as spores and later became active as the temperature cooled. As highlighted previously, closely related species have been isolated from high saline environments, particularly in the dual temperature experiments. Due to the low water availability, it is likely that adaptations to high saline environments would also be advantageous in the study presented here, and in the repository, even though the groundwater used in these experiments is of low salinity.

4.2. Putative activities of the indigenous bacterial community

Within the bacterial communities presented there were ASVs most similar to some known IRBs; *Bacillus subterraneus* is capable of dissimilatory iron reduction (Kanos et al., 2002), as is *C. beijerinckii* (Dobbin et al., 1999). Previous work (Gilmour et al., 2021) investgated the iron-reducing capablity of this community that was found to be equal to that of *Shewanella oneidensis,* a model iron-reducer. Including dissimilatory iron-reduction by known IRBs, it was thought that interactions between fermentation products (acetate and hydrogen) and iron minerals also contributed to Fe (III) reduction to Fe (II). Reduction of iron in iron-containing silicate minerals in the MX80 bentonite could result in a loss of silica and transformation to non-swelling minerals, making the clay more prone to weathering (Pusch and Kasbohm, 2002) and causing a decrease in the PI. This alteration would decrease the ability of the clay to act as an effective barrier to nuclear waste. Although abiotically this transformation is slow and requires high temperatures to proceed, biogenic dissolution of smectite does not have the same requirements (Kim, 2012). Smectite to illite transformations occur biogenically as dissolution of smectite and reprecipitation

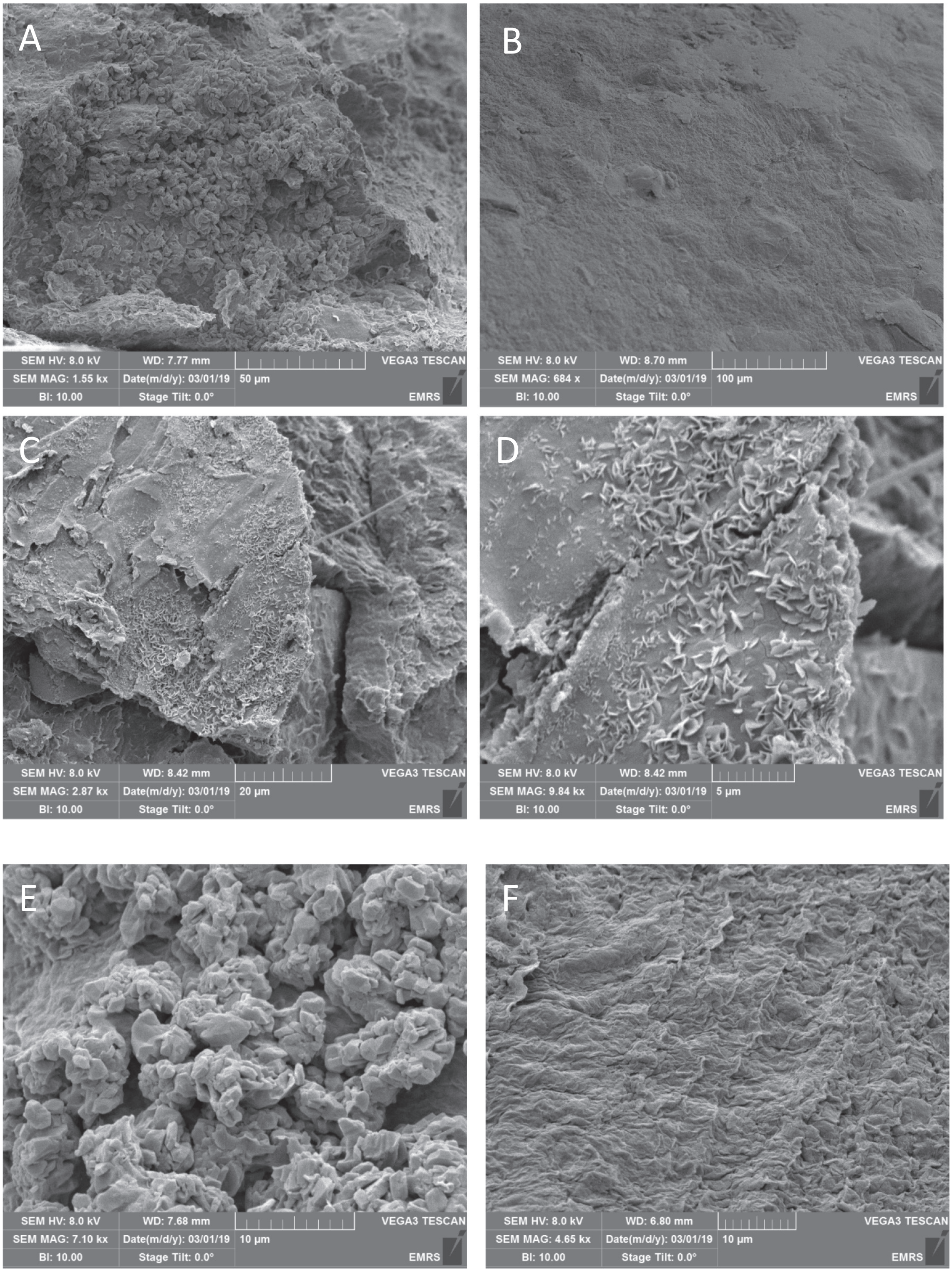

Fig. 5. SEM images of MX80 bentonite following desiccation tolerance experiments at 40 °C (A). No mineralization was observed on the corresponding abiotic control (B). Mineral formation from experiments at 70 °C was observed when microbes were present (C. D). Mineral precipitation was observed on MX80 bentonite from dual temperature experiments (E), the abiotic control was smooth (F).

as K / Al illite – this has been shown to be catalysed by IRBs reducing Fe (III) present in silicate minerals (Kim, 2012; Fang et al., 2017; Bradbury et al., 2014). There is also evidence that the role of organic secretions in iron reduction will lead to smectite - illite transformations (Kim, 2012).

Also present in the community when incubated at 40 °C were ASVs most similar to *C. subterminale,* which although connected to iron reduction has not been shown conclusively to reduce iron (Kato et al., 2015). Some species of *Romboutsia* (a genus belonging to the class *Clostridia*) are also known to reduce iron (Gerritsen et al., 2017), however, it is not possible to know if those particular species were present here.

Even in the community from the 70 °C experiments there were ASVs corresponding to species with a putative iron-reducing ability. *Lactobacillus*

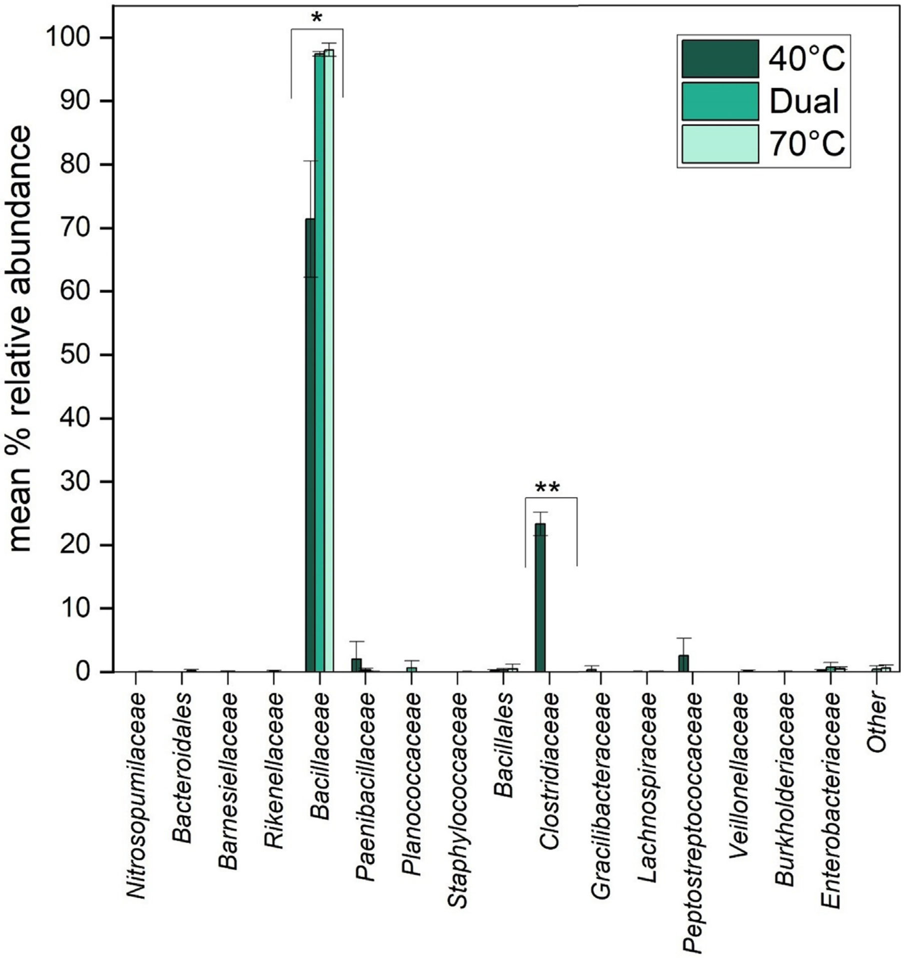

Fig. 6. Partial 16S rRNA gene-based community structure analysis of MX80 bentonite enriched iron-reducing / fermenting microbial community following desiccation tolerance experiments. The relative abundance (%) of the taxonomic group sequences in amplicon libraries are shown at the lowest taxonomic level to which the constituent ASVs were assignable. "Other" refers to species <0.02% relative abundance. Error bars represent standard error ($n = 3$) and stars represent statistically significant differences between different temperature treatments (*, $p = 0.0236$; ** $p = 0.0027$).

fermentim is able to reduce iron (González et al., 2017) and, *Bacillus licheniformis* is implicated in iron-reduction, but only in the presence of oxygen (McLean et al., 1992). Additionally, *Lysinibacillus halotolerans* has been shown to adhere to iron surfaces and, therefore, it is likely that there is some interaction and possibly iron reduction potential in this organism (Douterelo et al., 2014). Likewise, *Paenibacillus etheri* has been implicated in iron reduction (Loyaux-Lawniczak et al., 2019).

Additionally, some of these species are known to interact with silica. Both *P. aeruginosa* and *B. licheniformis* activity has been shown to lead to loss of silica from clays (Mohanty et al., 1990; Radhapriya et al., 2015). Such a change in mineralogy could result in a decrease to the swelling ability of MX80 bentonite.

It is well known that fermenting bacteria, such as firmicutes identified in these microbial communities can produce volatile fatty acids (VFAs), which can further interact with metals such as iron (Parrello et al., 2016) and support the growth of other members of the community (Bengtsson et al., 2015; Svensson et al., 2011; Gilmour et al., 2021). This process may have aided in the survival of non-fermenting species in the community in these experiments. Possible VFA production, from either carbon in the clay or the breakdown of cell biomass in the inoculum, in addition to the acetate added, may also lead to increases in iron-reduction (Parrello et al., 2016; Bengtsson et al., 2017; Svensson et al., 2011). This iron reduction could in turn could cause a release of silica from iron-containing silicate minerals (Bennett et al., 2001). Indeed, Hiebert and Bennett (1992) found that organic acid producti members of the communon by fermentative bacteria such as those identified here, increased the rate of silicate weathering from feldspar and quartz minerals. Furthermore, CO_2 is produced by acetogenic bacteria (*C. beijerinckii, C. magnum; C. huakuii*). In this environment, the CO_2 produced could also contribute to a decrease in pH and further silicate weathering (eq. 1) resulting in loss of silica through production of silicic acid and aqueous bicarbonate. MX80 is composed of 81.4%wt. montmorillonite (31% wt. silicon) and 4% wt. iron (Karnland, 2010). Changes to these minerals could therefore result in widespread mineralogical changes to the structure and properties of the clay.

$$4H_2O + 2CO_2 + SiO_2 = 2HCO_3- + 2H^+ + H_4SiO_4 \quad [1]$$

4.3. Potential corrosion protection afforded by microbial activity

As indicated in the results, there was significantly less corrosion of the surface of the steel coupon when microbes were present. Although this surface based assessment did not account for the depth of corrosion, or the overall weight loss from the steel coupon, it does suggest that microbial presence directly or indirectly limited contact of oxidants with the steel surface. This is likely due to bacteria utilizing all available oxygen in the system through aerobic respiration. This would lead to anoxic corrosion processes, which although slower, may include localised corrosion such as hydrogen embrittlement (Yang et al., 2019). However, as Leupin et al. (2017) suggests, microbes within the repository will utilise gases (such as residual oxygen or hydrogen produced through corrosion reactions), which could aid in accelerating the transition to anaerobic conditions therefore decreasing early corrosion of the waste canister and limiting hydrogen embrittlement, although in situ studies by Stroes-Gascoyne et al. (2000) suggest that microbial presence has no significant effect on gas composition. However, it may be that microbial hydrogen and CO_2 products are being utilised elsewhere in the repository – such as in iron-reduction or weathering of silicate minerals (eq. 1), rather than not being produced or accumulated.

There is evidence of mineral precipitation (low-cristobalite, and iron oxides such as magnetite) at the clay / steel interface when microbes were present, as seen in SEM images. This mineralogical change was contradicted by the photographs of the steel surface that indicate more extensive corrosion (and thereby iron oxides) in the sterile experiments. An explanation for this is that microbial presence increases the ability of rust products to diffuse into the clay, or that the iron oxides observed in the microbial experiments are from the reduction of minerals within the clay, rather than from the steel. This explanation is supported by the decrease in PI observed in microbial experiments.

Magnetite, lepidocrocite and goethite are all common corrosion products (Antunes et al., 2003). Whilst magnetite is not known to inhibit corrosion (Dong et al., 2000; Boin et al., 2000), other iron oxides may contribute to corrosion protection (Necib et al., 2017). Nitrate-reducing bacteria such as those present here (*P. etheri, Lactobacillus halotolerans, Bacillus korlensis* and *B. licheniformis* (Zhang et al., 2009; Loyaux-Lawniczak et al., 2019; Kong et al., 2014; Albert et al., 2005; Lee et al., 2017)) have also been implicated in rust formation to inhibit corrosion (Etique et al., 2014). The low porosity of these rust layers inhibits electrons from reaching the steel surface and therefore prevents further corrosion. In this study, this method of protection may have been limited due to the reduced activity of the microbes under the unfavourable conditions. Limited corrosion took place across all experiments due to the low water / oxygen conditions, but there is potential for these layers to develop in the repository over time.

4.4. Potential mineralogical alterations to MX80 bentonite

The most notable differences between the biotic and abiotic clay samples were the presence of iron oxides at 40 °C and 70 °C. Although samples for XRD analysis were taken from throughout the clay, it is not clear if these iron oxides are steel corrosion products that have moved into the clay or are from structural iron within the MX80 bentonite. Sodium iron oxide was also observed in the XRD analysis and is likely the product of microbially-influenced iron-reduction (Usman et al., 2012). The lack of moisture may have induced the formation of sodium iron-oxide through an increase in salinity. Similar iron-oxides have been identified by Leban and Kosec (2017) who found that goethite was replaced by magnetite or lepidocrocite formed on mild steel, by comparing this to results presented here, the mineral formation seen in Fig. 5B is likely lepidocrocite. The presence of IRBs may contribute to magnetite and goethite formation as they are produced as secondary minerals during dissimilatory iron-reduction coupled to oxidation of organic matter (Lovley, 1991; Shimizu et al., 2013). Iron-reduction, to form secondary magnetite, can also be catalysed by the presence of Fe (II), which accounts for 0.8% wt. of the total iron in MX80 bentonite (Karnland, 2010). Therefore, there is another route in which abiotic iron-reduction to produce minerals such as magnetite may have progressed (Malik et al., 2016).

Magnetite was observed in the abiotic experiments at 70 °C and one possible explanation for this is that drying can inadvertently cause magnetite formation (Schwertmann and Murad, 1983; Lovley et al., 1987). As these samples have dried out the most during the experiment (Fig. 3), it is possible that this caused increased abiotic magnetite formation via iron-reduction. As can be seen in the PI results, the higher temperatures did correlate with minor decreases to clay plasticity, which can be attributed to abiotic iron-reduction to non-swelling minerals.

There were no iron oxides observed in the dual temperature experiments, either with or without microbes. A possible explanation for this is that the microbes present were not active for long enough to promote any widespread alterations. These samples had the lowest number of ASVs identified and the community does not contain any known iron-reducers. Whilst there are plenty of fermentative bacteria present, they are all spore-formers. Those bacteria that would have been active at 40 °C have likely been lost at 70 °C. This lack of iron-oxides could be an indication that no mineralogical changes have occurred on iron-containing silicate minerals. This conclusion is reflected in the PI of MX80 bentonite.

There were significant decreases in PI of MX80 bentonite from biotic experiments at 40 °C and 70 °C. This lower PI reflects the experiments that had putative IRBs in their microbial community. Furthermore, the SEM images of these experiments showed the presence of iron-oxides, which were also identified in XRD. Similar decreases in PI following exposure to heat were seen in (Davies et al., 2018). The decrease in PI is likely due to formation of non-swelling Fe (II) minerals and possibly a loss of silica from the clay matrix as a consequence of iron-reduction (Flórez-Góngora et al., 2020).

In terms of the repository, a higher PI is advantageous because it indicates that the MX80 bentonite will respond to changes in moisture content whilst remaining an effective barrier (Wilson et al., 2010). The decrease in PI reported here was largely due to a lower liquid limit, which could result in the canister sinking into the clay during periods of high moisture content. Further geomechanical tests were not possible due to the volume of clay used in these experiments. However, previous experiments by Svensson et al. (2011) detected a significant difference in swelling pressure before and after bentonite was exposed to high temperatures, although, that experiment did not consider microbial activity or specifically the resulting iron redox states that may have contributed to these changes. Likewise, experiments by Davies et al. (2018) found that incubating highly compacted MX80 bentonite at elevated temperatures with steel decreased both the plasticity and swell index. Indeed, the results show that PI continued to decrease as time increased, however, these experiments also did not consider the possibility of microbially-influenced mineralogical changes.

4.5. Conclusions

This experiment aimed to investigate the survivability of microbes indigenous to MX80 bentonite under desiccated, high temperature conditions. Additionally, the mineralogical changes to the clay associated to the microbial presence were assessed and changes to the geomechanical properties of the clay were considered. Some species present in the viable indigenous iron-reducing community of MX80 bentonite can survive the highest temperatures expected at the host rock / clay interface in low water conditions. These microbes are largely spore-forming species. However, if limited activity can occur in areas where clay swelling has not fully closed gaps e.g., at the host rock wall, biologically- influenced iron-reduction may take place due to the presence of IRBs. This biogenic process may lead to a decrease in plasticity through associated loss of silica from the clay matrix which could alter the ability of the MX80 bentonite to act as barrier to nuclear waste. There is also evidence to support the conclusion that microbes can enter dormancy at 70 °C in order to survive to a more favourable habitat, however, some mesophiles cannot recover from exposure to this high temperature. Finally, there is likely utilisation of oxygen by aerobic microbial respiration, which acts to indirectly protect steel from corrosion. Further biogenic protection may occur and, taking into account the species identified in the community, this protection could be through formation of a low porosity rust layer or by biofilm formation.

Declaration of Competing Interest

The authors declare that they have no known competing financial interests or personal relationships that could have appeared to influence the work reported in this paper.

Acknowledgements

The authors would like to thank EPSRC for funding this project and NU-OMICS (Northumbria University Omics Lab, DNA sequencing research facility) for their help in sequencing.

Appendix A. Supplementary data

Supplementary data to this article can be found online at https://doi.org/10.1016/j.scitotenv.2021.152660.

References

Albert, R.A., Archambault, J., Rosello-Mora, R., Tindall, B.J., Matheny, M., 2005. Bacillus acidicola sp. nov., a novel mesophilic, acidophilic species isolated from acidic sphagnum peat bogs in Wisconsin. International journal of systemic and evolutionary. Microbiology 55 (5). https://doi.org/10.1099/ijs.0.02337-0.

Antunes, A., Costa, I., Faria, D.L.A., 2003. Characterization of corrosion products formed on steels in the first months of atmospheric exposure. Mater. Res. 6, 3. https://doi.org/10.1590/S1516-14392003000300015.

Arlinger, J., Bengtsson, A., Edlund, J., Eriksson, L., Johansson, J., Lydmark, S., Rabe, L., Pedersen, K., 2013. Prototype repository – microbes in the retrieved outer section. Report P-13-16 Swedish Nuclear Fuel and Waste Management Co.

Aunqué, L.F., Gimeno, M.J., Gómez, J.B., Puigdomenech, I., Smellie, J., Tullborg, E.-L., 2006. Groundwater chemistry around a repository for spent nuclear fuel over a glacial cycle. Report TR-06-31 Swedish Nuclear Fuel and Waste Management Co.

Baker, A., Chambers, A., Jackson, C., 1997. Nirex 97 an assessment of the post-closure performance of a deep waste repository at Sellafield. Volume 3; the groundwater pathway. Technical Report no., Nirex-SR-S-97/012/3.

Bengtsson, A., Edlund, J., Hallbeck, B., Heed, C., Pedersen, K., 2015. Microbial sulphide-producing activity in MX-80 bentonite at 1750 and 2000 kg m–3 wet density. Report R-15-05 Swedish Nuclear Fuel and Waste Management Co.

Bennett, P.C., Rogers, J.R., Choi, W.J., Hiebert, F.K., 2001. Silicates, silicate weathering, and microbial ecology. Geomicrobiol. J. 18, 3–19. https://doi.org/10.1080/01490450151079734.

Boin, P.M.L., Odziemkowski, M.S., Reardon, E.J., Gillham, R.W., 2000. In situ identification of carbonate-containing green rust on iron electrodes in solutions simulating groundwater. J. Solut. Chem. 29, 10. https://doi.org/10.1023/A:1005103304964.

Börjesson, 2010. Design, production and initial state of the buffer. SKB Technical Report, Report TR-10-15 Swedish Nuclear Fuel and Waste Management Co.

Börgesson, L., Hedström, M., Holton, D., Metcalfe, R., Sandén, T., 2020. Bentonite in a high-temperature environment bentonite erosion. RWM Report no. RWM/Contr/20/029.

Bradbury, M.H., Berner, U., Curti, E., Hummel, W., Kosakowski, G., Thoenen, T., 2014. The long term geochemical evolution of the nearfield of the HLW repository. Technical Report TR-12-01 Nagra.

Institution, British Standards, 1990. BS EN ISO 1377:1990 Methods of Test for Soils for Civil Engineering Purposes. Part 2 Section 2.3, 3.4, 3.5.

Callahan, B.J., McMurdie, P.J., Rosen, M.J., Han, A.W., Johnson, A.J.A., Holmes, S.P., 2016. DADA2: high resolution sample inference from illumina amplicon data. Nat. Methods 13 (7), 581–583. https://doi.org/10.1038/nmeth.3869.

Caporaso, J.G., Kuczynski, J., Stombaugh, J., Bittinger, K., Bushman, F.D., Costello, E.K., Fierer, N., Gonzalez, Pena A., Goodrich, J.K., Gordon, J.I., Huttley, G.A., Kelley, S.T., Knights, D., Koenig, J.E., Ley, R.E., Lozupone, C.A., McDonald, D., Muegge, B.D., Pirrung, M., Reeder, J., Sevinsky, J.R., Turnbaugh, P.J., Walters, W.A., Widmann, J., Yatsunenko, T., Zaneveld, J., Knight, R., 2010. QIIME allows analysis of high-throughput community sequencing data. Nat. Methods 7 (5), 335–336. https://doi.org/10.1038/nmeth.f.303.

Chi, Fru E., Athar, R., 2008. In situ bacterial colonization of compacted bentonite under deep geological high-level radioactive waste repository conditions. Appl. Microbiol. Biotechnol. 79 (3), 499–510. https://doi.org/10.1007/s00253-008-1436-z.

Davies, C.W., Davie, C.T., Edward, C.A., White, M.L., 2018. Physicochemical and geotechnical alterations to MX-80 bentonite at the waste canister Interface in an engineered barrier system. Geosciences 7 (3), 69. https://doi.org/10.3390/geosciences7030069.

Dobbin, P.S., Carter, J.P., San, Juan C., von Hobe, M., Powell, A.K., Richardson, D.J., 1999. Dissimilatory Fe(III) reduction by Clostridium beijerinckii isolated from freshwater sediment using Fe(III) maltol enrichment. FEMS Microbiol. Lett. 176 (1), 131–138. https://doi.org/10.1111/j.1574-6968.1999.tb13653.x.

Dong, H., Fredrickson, J.K., Kennedy, D.W., Zachara, J.M., Kukkadapu, R.K., Onstott, T.C., 2000. Mineral Transformation Associated With the Microbial Reduction of Magnetite. 143. US Department of Energy.

Douterelo, I., Husband, S., Boxall, J.B., 2014. The bacteriological composition of biomass recovered by flushing an operational drinking water distribution system. Water Res. 54, 100–114. https://doi.org/10.1016/j.watres.2014.01.049.

Etique, M., Jorand, F.P.A., Zegeye, A., Grégoire, B., Despas, C., Ruby, C., 2014. Abiotic process for Fe(II) oxidation and green rust mineralization driven by a heterotrophic nitrate reducing bacteria (Klebsiella mobilis). Environ. Sci. Technol. 48 (7), 3742–3751. https://doi.org/10.1021/es403358v.

Fan, Y.Y., Li, B.B., Yang, Z.C., Cheng, Y., Liu, D., Yu, H., 2018. Abundance and diversity of iron reducing bacteria communities in the sediments of a heavily polluted freshwater lake. Appl. Microbiol. Biotechnol. 102, 10791–10801. https://doi.org/10.1007/s00253-018-9443-1.

Fang, Q., Churchman, G.J., Hong, H., Chen, Z.Q., Liu, J., Yu, J., Han, W., Wang, C., Zhao, L., Furnes, H., 2017. New insights into microbial smectite illitization in the permo-triassic boundary K-bentonites, South China. Appl. Clay Sci. 140, 96–111. https://doi.org/10.1016/j.clay.2017.01.029.

Felsenstein, J., 1987. Phylogenies and the comparative method. Am. Nat. 125 (1), 1–15.

Flórez-Góngora, C.H., Garzón-Peña, A.T., Molina-Giraldo, R.D., 2020. Testing stabilization of high-plasticity clays used in sloping terrain by adding sodium silicate. J. Phys. Conf. Ser. 1587, 012036.

Fraser Harris, A.P., Kolditz, O., Haszeldine, R.S., McDermott, C.I., 2015. Modelling groundwater flow changes due to thermal effects of radioactive waste disposal at a hypothetical repository site near Sellafield, UK. Environ Earth Sci 74, 1589–1602. https://doi.org/10.1007/s12665-015-4156-6.

Gerritsen, J., Hornung, B., Renckens, B., van Hijum, S., Martins Dos Santos, V., Rijkers, G.T., Schaap, P.J., de Vos, W.M., Smidt, H., 2017. Genomic and functional analysis of romboutsia ilealis CRIBT reveals adaptation to the small intestine. PeerJ 5, e3698.

Gilmour, K.A., Davie, C.T., Neil, G., 2021. An indigenous iron-reducing microbial community from MX80 bentonite - a study in the framework of nuclear waste disposal. Appl. Clay Sci. 205, 106039. https://doi.org/10.1016/j.clay.2021.106039.

Glatstein, D.A., Francisca, F.M., 2014. Hydraulic conductivity of compacted soils controlled by microbial activity. Environ. Technol. 35 (13–16), 1886–1892. https://doi.org/10.1080/09593330.2014.885583.

González, A., Gálvez, N., Martín, J., Reyes, F., Pérez-Victoria, I., Dominguez-Vera, J.M., 2017. Identification of the key excreted molecule by lactobacillus fermentum related to host iron absorption. Food Chem. 228, 374–380. https://doi.org/10.1016/j.foodchem.2017.02.008.

Hallbeck, L., Pedersen, K., 2012. Culture-dependent comparison of microbial diversity in deep granitic groundwater from two sites considered for a swedish final repository of spent nuclear fuel. FEMS Microbiol. Ecol. 81, 66–77. https://doi.org/10.1111/j.1574-6941.2011.01281.x.

Hiebert, F.K., Bennett, P.C., 1992. Microbial control of silicate weathering in organic-rich ground water. Science 258 (5080), 278–281. https://doi.org/10.1126/science.258.5080.278.

Horwell, C.J., Williamson, B.J., Llewellin, E.W., Damby, D.E., Le Blond, J.S., 2013. The nature and formation of cristobalite at the Soufrière Hills volcano, Montserrat: implications for the petrology and stability of silicic lava domes. Bull. Volcanol. 75, 696. https://doi.org/10.1007/s00445-013-0696-3.

IAEA, 2018. Status and Trends in Spent Fuel and Radioactive Waste Management. IAEA Nuclear Energy Series, No. NW-T-1.14.

Jalique, D.R., Stroes-Gascoyne, S., Hamon, C.J., Priyanto, D.G., Kohle, C., Evenden, W.G., Wolfaardt, G.M., Grigoryan, A.A., McKelvie, J., Korber, D.R., 2016. Culturability and diversity of microorganisms recovered from an eight-year old highly-compacted, saturated MX-80 Wyoming bentonite plug. Appl. Clay Sci. 126, 245–250. https://doi.org/10.1016/j.clay.2016.03.022.

Jönsson, B., Åkesson, T., Jönsson, B., Meehdi, S., Janiak, J., Wallenberg, R., 2009. Structure and forces in bentonite MX-80. Report TR-09-06 Swedish Nuclear Fuel and Waste Management Co.

Kanos, S., Greene, A.C., Patel, B.K.C., 2002. Bacillus subterraneus sp. Nov., an iron- and manganese-reducing bacterium from a deep subsurface australian thermal aquifer. International journal of systemic and evolutionary. Microbiology 52 (3). https://doi.org/10.1099/00207713-52-3-869.

Karnland, O., 2010. Chemical and mineralogical characterization of the bentonite buffer for the acceptance control procedure in a KBS-3 repository. Report, TR-10-60 Swedish Nuclear Fuel and Waste Management Co.

Kato, S., Yumoto, I., Kamagata, Y., 2015. Isolation of acetogenic bacteria that induce biocorrosion by utilizing metallic iron as the sole electron donor. Appl. Environ. Microbiol. 81 (1), 67–73. https://doi.org/10.1128/AEM.02767-14.

Kim, J., 2012. Overviews of biogenic smectite-to-illite reaction. Clay Sci. 16 (1), 9–13. https://doi.org/10.11362/jcssjclayscience.16.1_9.

Kim, J., Dong, H., Seabaugh, J., Newell, S.W., Eberl, D.D., 2004. Role of microbes in the smectite-to-illite reaction. Science 303 (5659), 830–832. https://doi.org/10.1126/science.1093245.

Kiviranta, L., Kumpulainen, S., 2011. Quality control and characterization of bentonite materials. POSIVA 2011–2084.

Kong, D., Wang, Y., Zhao, B., Li, Y., Song, J., Zhai, Y., Zhang, C., Wang, H., Chen, X., Zhao, B., Ruan, Z., 2014. Lysinibacillus halotolerans sp. nov., isolated from saline-alkaline soil. International Journal of Systemic and Evolutionary Microbiology 64 (8). https://doi.org/10.1099/ijs.0.061465-0.

Konhauser, K., 2007. Introduction to Geomicrobiology. Blackwell ch4 and 5.

Kotelnikova, S., Pedersen, K., 1998. Distribution and activity of methanogens and homoacetogens in deep granitic aquifers at Äspö hard rock laboratorySweden. FEMS Microbiology Ecology 26 (2), 121–134. https://doi.org/10.1111/j.1574-6941.1998.tb00498.x.

Kozich, J.J., Westcott, S.L., Baxter, N.T., Highlander, S.K., Schloss, P.D., 2013. Development of a dual-index sequencing strategy and curation pipeline for analyzing amplicon sequence data on the MiSeq illumina sequencing platform. Appl. Environ. Microbiol. 79 (17), 5112–5120. https://doi.org/10.1128/AEM.01043-13.

Kuleshova, M.L., Danchenko, N.N., Sergeev, V.I., Shimko, T.G., Malashenko, Z.P., 2014. The properties of bentonites as a material for sorptive barriers. Mosc. Univ. Geol. Bull. 69, 356–364. https://doi.org/10.3103/S0145875214050044.

Kyle, J.E., Eydal, H.S.C., Ferris, F.G., Pedersen, K., 2008. Viruses in granitic groundwater from 69 to 450 m depth of the Äspö hard rock laboratory, Sweden. ISME J 2, 571–574. https://doi.org/10.1038/ismej.2008.18.

Landlot, D., Davenport, A., Payer, J., Shoesmith, D., 2009. A Review of Materials and Corrosion Issues Regarding Canisters for Disposal of Spent Fuel and High-level Waste in Opalinus Clay. Report TR-09-02, Nagra.

Lantenois, S., Lanson, B., Muller, F., Bauer, A., Jullien, M., Plançon, A., 2005. Experimental study of smectite interaction with metal fe at low temperature: 1Smectite destabilization. Clays Clay Miner. 53, 597–612. https://doi.org/10.1346/CCMN.2005.0530606.

Leban, M.B., Kosec, T., 2017. Characterization of corrosion products formed on mild steel in deoxygenated water by Raman spectroscopy and energy dispersive X-ray spectrometry. Eng. Fail. Anal. 79, 940–950. https://doi.org/10.1016/j.engfailanal.2017.03.022.

Lee, C., Kim, J.Y., Song, H.S., Kim, Y.B., Choi, Y.E., Yoon, C., Nam, Y., Roh, S.W., 2017. Genomic analysis of bacillus licheniformis CBA7126 isolated from a human fecal sample. Front. Pharmacol. 8, 724. https://doi.org/10.3389/fphar.2017.00724.

Leupin, O.X., Bernier-Latmani, R., Bagnoud, A., Moors, H., Leys, N., Wouters, K., Stroes-Gascoyne, S., 2017. Fifteen years of microbial investigation in opalinus clay at the mont Terri rock laboratory (Switzerland). Swiss J. Geosci. 110 (1), 343–354. https://doi.org/10.1007/s00015-016-0255-y.

Lovley, D.R., Stolz, J.F., Nord Jr., G.L., Phillips, E.J.P., 1987. Anaerobic production of magnetite by a dissimilatory iron-reducing microorganism. Nature 330, 252–254. https://doi.org/10.1038/330252a0.

Lovley, D.R., 1991. Magnetite formation during microbial dissimilatory iron reduction. Iron Minerals, 151–166 https://doi.org/10.1007/978-1-4615-3810-3_11.

Loyaux-Lawniczak, S., Vuilleumier, S., Geoffroy, V.A., 2019. Efficient reduction of iron oxides by paenibacillus spp. Strains isolated from tropical soils. Geomicrobiol J. 36 (5), 423–432. https://doi.org/10.1080/01490451.2019.1566415.

Malik, S., Hewitt, I., Powell, A., 2016. Electron microscopy of anionic surfactant-directed synthesis of magnetite nanoparticles. Chem. J. Moldova 11, 69–73. https://doi.org/10.19261/cjm.2016.11(1).09.

Marshall, M.H.M., McKelvie, J.R., Simpson, A.J., Simpson, M.J., 2015. Characterization of natural organic matter in bentonite clays for potential use in deep geological repositories for used nuclear fuel. Appl. Geochem. 54, 43–53. https://doi.org/10.1016/j.apgeochem.2014.12.013.

Masurat, P., Eriksson, S., Pedersen, K., 2010. Evidence of indigenous sulphate-reducing bacteria in commercial Wyoming bentonite MX80. Appl. Clay Sci. 47, 51–57. https://doi.org/10.1016/j.clay.2008.07.002.

McLean, R.J., Beauchemin, D., Beveridge, T.J., 1992. Influence of oxidation state on iron binding by bacillus licheniformis capsule. Appl. Environ. Microbiol. 58 (1), 405–408. https://doi.org/10.1128/aem.58.1.405-408.1992.

Mohanty, B., Ghosh, S., Mishra, A., 1990. The role of silica in bacillus licheniformis. J. Appl. Bacteriol. 68, 55–60. https://doi.org/10.1111/J.1365-2672.1990.TB02548.X.

Morgado, L., Fernandes, A.P., Dantas, J.M., Silva, M.A., Salgueiro, C.A., 2012. On the road to improve the bioremediation and electricity-harvesting skills of geobacter sulfurreducens: functional and structural characterization of multihaem cytochromes. Biochem. Soc. Trans. 40 (6), 1295–1301. https://doi.org/10.1042/BST20120099.

Nda, 2010. Summary of generic designs. Geological Disposal NDA Report No: NDA/RWMD/054.

NDA, 2016. Geological disposal waste package evolution status report December 2016. NDA Report No: DSSC/451/01.

Necib, S., Diomidis, M., Keech, P., Nakayama, M., 2017. Corrosion of carbon steel in clay environments relevant to radioactive waste geological disposals, mont Terri rock laboratory (Switzerland). Swiss J. Geosci. 110 (1), 329–342. https://doi.org/10.1007/s00015-016-0259-7.

Neretnieks, I., Liu, L., Moreno, L., 2009. Mechanisms and models for bentonite erosion. Report TR-09-35 Swedish Nuclear Fuel and Waste Management Co.

Parrello, D., Zegeye, A., Mustin, C., Billard, P., 2016. Siderophore-mediated iron dissolution from nontronites is controlled by mineral cristallochemistry. Frontiers Microbiology 7, 423. https://doi.org/10.3389/fmicb.2016.00423.

Patakova, P., Branska, B., Sedlar, K., Vasylkivska, M., Jureckova, K., Kolek, J., Koscova, P., Provaznik, I., 2019. Acidogenesis, solventogenesis, metabolic stress response and life cycle changes in Clostridium beijerinckii NRRL B-598 at the transcriptomic level. Sci. Rep. 9, 1371. https://doi.org/10.1038/s41598-018-37679-0.

Pedersen, K., 2012. Subterranean microbial populations metabolise hydrogen and acetate under in situ conditions in granitic groundwater at 450m depth in the Äspö Hard Rock Laboratory, Sweden. FEMS Microbiology Ecology 81 (1), 217–229. https://doi.org/10.1111/j.1574-6941.2012.01370.x.

Pedersen, K., Bengtsson, A., Blom, A., Johansson, L., Taborowski, T., 2017. Mobility and reactivity of sulphide in bentonite clays – implications for engineered bentonite barriers in geological repositories for radioactive wastes. Elsevier 146, 495–502. https://doi.org/10.1016/j.clay.2017.07.003.

Poulain, S., Sergeant, C., Simonoff, M., Le Marrec, C., Altmann, S., 2008. Microbial investigations in opalinus clay, an agrillaceous formation under evaluation as a potential host rock for a radioactive waste repository. Geomicrobiol J. 25 (5), 240–249. https://doi.org/10.1080/01490450802153314.

Povedano-Priego, C., Jroundi, F., Lopez-Fernandez, M., Shrestha, R., Spanek, R., Martín-Sánchez, I., Villar, M.V., Ševců, A., Dopson, M., Merroun, M.L., 2020. Deciphering indigenous bacteria in compacted bentonite through a novel and efficient DNA extraction method: insights into biogeochemical processes within the deep geological disposal of nuclear waste concept. J. Hazard. Mater. 408, 124600. https://doi.org/10.1016/j.jhazmat.2020.124600.

Pusch, R., Kasbohm, J., 2002. Alteration of MX-80 by hydrothermal treatment under high salt content conditions. Report TR-02-06 Swedish Nuclear Fuel and Waste Management Co.

Radhapriya, P., Ramachandran, A., Anandham, R., Mahalingam, S., 2015. Pseudomonas aeruginosa RRALC3 enhances the biomass, nutrient and carbon contents of Pongamia pinnata seedlings in degraded Forest soil. PloS one 10 (10). https://doi.org/10.1371/journal.pone.0139881.

Rättö, M., Itävaara, M., 2012. Microbial activity in bentonite buffers. VTT Technology 20, 30.

RStudio Team, 2020. RStudio: Integrated Development for R. RStudio, PBC, Boston, MA http://www.rstudio.com/.

RWM, 2016. Geological disposal: generic Specification for waste packages containing high heat generating waste. WPSGD no. WPS/240/01.

Sahin, U., Eroğlu, S., Sahin, F., 2011. Microbial application with gypsum increases the saturated hydraulic conductivity of saline–sodic soils. Appl. Soil Ecol. 48 (2), 247–250. https://doi.org/10.1016/j.apsoil.2011.04.001.

Saitou, N., Nei, M., 1987. The neighbour-joining method: a new method for reconstructing phylogenetic trees. Mol. Biol. Evol. 4 (4), 406–425. https://doi.org/10.1093/oxfordjournals.molbev.a040454.

Sauzeat, E., Villiéras, T.F., François, M., Pelletier, M., Barrés, O., Yvon, J., Guillaume, D., Dubbessy, J., Pfeiffert, C., Ruck, R., Cathelineau, M., 2001. Caractérisation minéralogique, cristallochimique et texturale de l'argile MX-80. ANDRA Technical Report 21000763.

Schäfer, T., Geckeis, H., Bouby, M., Fanghänel, T., 2004. U, Th, Eu and colloid mobility in a granite fractureunder near-natural flow conditions. Radiochim. Acta 92, 731–737.

Schwertmann, U., Murad, E., 1983. Effect of pH on the formation of goethite and hematite from ferrihydrite. Clay Clay Miner. 31 (4), 277–284. https://doi.org/10.1346/CCMN.1983.0310405.

Sellin, P., Leupin, O.X., 2013. The use of clay as an engineered barrier in radioactive-waste management – a review. GeoSci. World 61 (6), 477–498. https://doi.org/10.1346/CCMN.2013.0610601.

Shimizu, M., Zhou, J., Schröder, C., Obst, M., Kappler, A., Borch, T., 2013. Dissimilatory reduction and transformation of ferrihydrite-humic acid coprecipitates. Environ. Sci. Technol. 47, 13375–13384. https://doi.org/10.1021/es402812j.

Singh, V.K., Singh, A.L., Singh, R., Kumar, A., 2018. Iron oxidizing bacteria: insights on diversity, mechanism of iron oxidation and role in management of metal pollution. Environ. Sustain. 1, 221–231. https://doi.org/10.1007/s42398-018-0024-0.

Smart, N.R., Reddy, B., Rance, A.P., Nixon, D.J., Frutschi, M., Bernier-Latmani, R., Diomidis, N., 2017. The anaerobic corrosion of carbon steel in compacted bentonite exposed to natural opalinus clay porewater containing native microbial populations. Corros. Eng. Sci. Technol. 52 (1), 101–112. https://doi.org/10.1080/1478422X.2017.1315233.

Stroes-Gascoyne, S., Hamon, C.J., Vilks, P., Gierszewski, P., 2002. Microbial, redox and organic characteristics of compacted clay-based buffer after 6.5 years of burial at AECL's underground research laboratory. Appl. Geochem. 17, 1287–1303. https://doi.org/10.1016/S0883-2927(02)00020-3.

Stroes-Gascoyne, S., Hamon, C.J., Vilks, P., 2000. Microbial analysis of the isothermal test at AECL's Underground Research Laboratory.Prepared by Atomic Energy of Canada Limited for Ontario Power Generation. Report 06819-REP-01200-10023-R00. Ontario Power Generation Nuclear Waste Management Division.

Stroes-Gascoyne, S., Hamon, C.J., Maak, P., 2011. Limits to the use of highly compacted bentonite as a deterrent for microbially influenced corrosion in a nuclear fuel waste repository. Phys. Chem. Earth 36, 1630–1638. https://doi.org/10.1016/j.pce.2011.07.085.

Stone, W., Kroukamp, O., Moes, A., McKelvie, J., Korber, D.R., Wolfaardt, G.M., 2016. Measuring microbial metabolism in atypical environments: bentonite in used nuclear fuel storage. J. Microbiol. Methods 120, 79–90. https://doi.org/10.1016/j.mimet.2015.11.006.

Stucki, J.W., Lee, K., Zhang, L., Larson, R.A., 2009. Effects of iron oxidation states on the surface and structural properties of smectites. Pure Appl. Chem. 74, 2145–2158. https://doi.org/10.1351/pac200274112145.

Suttle, C.A., 2007. Marine viruses: major players in the global ecosystem. Nat. Rev. Microbiol. 5, 801–812. https://doi.org/10.1038/nrmicro1750.

Svemar, C., Johanneson, L.E., Grahm, P., Svensson, D., Kristensson, O., Lönnqvist, M., Nilsson, U., 2016. Opening and retrieval of outer section of Prototype Repository at Äspö Hard Rock Laboratory. Report TR-13-22 Swedish Nuclear Fuel and Waste Management Co.

Svensson, D., Dueck, A., Nilsson, U., Olsson, S., Sanden, T., Lydmark, S., Jagerwall, S., Pedersen, K., Hansen, S., 2011. Status of the ongoing laboratory investigation of reference materials and test package 1. Report TR-11-06 Swedish Nuclear Fuel and Waste Management Co.

Urios, L., Marsal, F., Pelligrini, D., Magot, M., 2012. Microbial diversity of the 180 million-year-old toarcian argillite from tounemireFrance. Appl. Geochem. 27 (7), 1442–1450. https://doi.org/10.1016/j.apgeochem.2011.09.022.

Uroz, S., Calvaruso, C., Turpault, M.-P., Frey-Klett, P., 2009. Mineral weathering by bacteria: ecology, actors and mechanisms. Trends Microbiol. 17, 378–387. https://doi.org/10.1016/j.tim.2009.05.004.

Usman, M., Hanna, K., Abdelmoula, M., Zegeye, A., Faure, P., Ruby, C., 2012. Formation of green rust via mineralogical transformation of ferric oxides (ferrihydrite, goethite and hematite). Appl. Clay Sci. 64, 38–43. https://doi.org/10.1016/j.clay.2011.10.008.

Wang, S., Xu, D., Wang, B., Sheng, L.Y., Han, E., Dong, C., 2016. Effect of solution treatment on stress corrosion cracking behavior of an as-forged Mg-Zn-Y-zr alloy. Sci. Rep. 6, 29471. https://doi.org/10.1038/srep29471.

West, J., McKinley, I.G., Stroes-Gascoyne, S., 2002. Microbial effects on waste repository materials. Interactions of Microorganisms with Radionuclides https://doi.org/10.1016/S1569-4860(02)80038-9 ch9.

Wilkins, M.J., Livens, F.R., Vaughan, D.J., Beadle, I., Lloyd, J.R., 2007. The influence of microbial redox cycling on radionuclide mobility in the subsurface at a low-level radioactive waste storage site. Geobiology 5, 293–301. https://doi.org/10.1111/j.1472-4669.2007.00101.x.

Wilson, J., Savage, D., Bond, A., Watson, S., Pusch, R., Bennett, D., 2010. Bentonite. NDA QRS-1378ZG-1.1.

Yang, Q., Toijer, E., Olsson, P., 2019. Analysis of radiation damage in the KBS-3 canister materials. Report TR-19-14 Swedish Nuclear Fuel and Waste Management.

Zhang, J., Wang, Y., Dai, J., Tang, Y., Yang, Q., Luo, X., Fang, C., 2009. Bacillus korlensis sp. nov., a moderately halotolerant bacterium isolated from a sand soil sample in China. International journal of systemic and evolutionary. Microbiology 59 (7). https://doi.org/10.1099/ijs.0.004879-0.